

1 **Red color is our draft reply and blue color lines are to be incorporated in the manuscript**

2
3 **Replies to Referee #1 comments/suggestions**

4
5 The present study investigates the atmospheric inversions over the Arabian sea observed by Satellite
6 observations (IASI and AIRS) and also a reanalysis data set of ERA interim. The analysis included
7 mean patterns, differences between active and break spells, weak and strong monsoons. Over all, the
8 paper is well written and the results are interesting. Even though there are reports on monsoon
9 inversions, the present study provides more details of the monsoon inversions. Therefore, I would
10 like to recommend the paper for publication. However, the authors may please examine the
11 following comments/ suggestions to improve the quality of the paper before it is published.

12 **First of all we wish to thank the reviewer for going through the manuscript, offering suggestions and**
13 **appreciating the contents of the work. We have taken care all the comments/suggestions made by the**
14 **three reviewers.**

15
16 1) The inversion values reported are positive. I am not able to appreciate why the values are positive.
17 How you subtracted? From higher level to lower level or other way? Another big issue is that you
18 have fixed the pressure levels same for all the days to retrieve temperature differences, which may
19 not be appropriate. You should examine each profile separately and identify the inversion layer and
20 then find the difference between the layers of the inversion. Therefore, for each profile, you have
21 track where is the inversion layer. Since the paper already documents that these layers can vary on
22 different dates, fixing the pressure levels is not appropriate.

23 **Reply: In the manuscript under Section 3 Methodology and Analysis procedure (Page 35284, Para 2)**
24 **- we have mentioned the way ΔT values are calculated. Conventionally the lapse rate is the**
25 **difference in Temperature at higher level minus Temperature at lower level and is a negative**
26 **quantity. However, in this study (as also in the work of N & R 1981) we have considered ΔT as**
27 **temperature difference between lower and higher level i.e. $\Delta T = T(950 \text{ hPa}) - T(850 \text{ hPa})$ which is**
28 **thus a positive quantity.**

29
30 **We have examined each and every individual profile to capture inversion height, depth and strength.**
31 **On the basis of this computation, Fig 3 has been generated. From this figure it could be ascertained**
32 **that in more than 95 % of cases, the inversion over Arabian sea is lying in the region 950 and 850**
33 **hPa. We have also mentioned in the text (Page 35285, lines 24 – 25) that “This level criteria (950 –**
34 **850 hPa) was arrived at after a detailed examination of ΔT at a few more level intervals (viz 1000 –**
35 **900 hPa, 1000 – 850 hPa, 850 – 750 hPa etc)”.**

36
37 **As we had to analyse a huge volume of data, we had to adopt an automatic criterion for**
38 **representing the inversion strength ΔT . An average ΔT for all the profiles in each 1 deg x 1 deg box**
39 **for each day was computed.**

40
41 **As mentioned in the manuscript, the upper / lower levels of inversion vary on individual days by a**
42 **small amount (~ 25 hPa). Even if the lower or upper level of inversion were at levels above 850 or**
43 **below 950 hPa by this small amount, the inversions would still be captured in the overall ΔT ,**
44 **though of a slightly lower magnitude.**

45
46 2) The ERA data is not showing any resemblance of that of observed in satellite data. I am not sure
47 therefore the discussion on ERA data is required. Recommendation: Revision

48 **Reply: As mentioned in the manuscript there is no ground truth (after 1979) over the Arabian sea to**
49 **compare with our results. Hence we have compared with ERA, the only available standard option of**
50 **comparison over AS. 3rd conclusion in our paper (Page 35297 lines 09-10) mentions about ERA's**

51 smoothed spatio temporal variability of ΔT . ERA – interim results match qualitatively with satellite
52 results, but vary in numbers.
53

54

55

---END---

56

57 **Replies to Referee #2 comments/suggestions**

58

59 **General comments**

60

61 This is a well-written and thorough study of the characteristics of monsoon inversions over the
62 Arabian Sea. The authors make use of a range of remote-sensing measurements validated against
63 available in situ observations and some reanalysis products. I have only a few minor
64 corrections/clarifications before this paper is suitable for publication.

65 **Reply:** First of all we wish to thank the reviewer for going through the manuscript and appreciating
66 the actual content of the work. We have taken care all the comments/suggestions made by the three
67 reviewers.

68

69 **Specific comments**

70

71 1) Page 35288 lines 14-15: "...somewhat varying strengths..." - and heights, at least of the inversion
72 base, though the top height is quite consistent.

73 **Reply:** We are modifying this sentence as suggested by referee as – A clear MI in the satellite profile
74 and ERA-Interim can be noticed though with somewhat varying strengths and base of inversion
75 height. However, the top height of inversion is consistent.

76

77 2) Page 35290 lines 4-11: You should also mention the low level vertical wind shear which is
78 prevalent in this region, particularly near the coast.

79 **Reply:** We have mentioned about low level vertical wind shear as suggested in the revised
80 manuscript.

81

82 3) Fig. 3 - is this a percentage of DAYS with a MI present or a percentage of the profiles measured
83 that had a MI? Please specify in the figure caption.

84 **Reply:** Yes, in the figure 3, the MIs shown are as percentage of Days. Caption is modified to:
85(d) August andPercentage occurrence of MI days (e) July

86

87 4) Page 35294 lines 8-9: How do you reach the conclusion that IASI "performs better" than AIRS?
88 I can't see how you judge this from the information you have provided. Please clarify.

89 **Reply:** We are modifying a few sentences in the manuscript (Page 35294, lines 5 - 9) as follows: A
90 distinct contrast between WAS and EAS with higher PO in the former region can be noticed. When
91 we consider EAS as a place to detect MI, AIRS observed always higher PO than IASI and almost
92 nothing is noticed in ERA Interim. Thus, we may infer that IASI is performing better than AIRS for
93 detecting MI (as ERA is in better agreement with IASI rather than with AIRS).

94

95 5) Page 35293 line 11: "...less value of..." replace with "a lower value of"

96 **Reply:** Complied with in the text.

97

98 ---END---

101 **Replies to Referee #3 comments/suggestions**

102 This is a detailed study on an important phenomenon, namely, temperature inversion over the Arabian
103 Sea during the boreal summer. Unique geographic location of the Arabian Sea and wind/pressure
104 field give rise to strong inversions, however, this has not received much attention. Authors combine
105 data from a variety of sources and have carried out a detailed analysis. I recommend its acceptance
106 after a revision accounting for the comments given below.

107
108 **First of all we wish to thank the reviewer for going through the manuscript and appreciating the**
109 **actual content of the work. We have taken care all the comments/suggestions made by the three**
110 **reviewers.**

111
112 1. P.35279, line 9. Colon (1964) also used dropsonde data

113 **Reply: We have reframed the sentence on Page 35279, line 9 as “from ship radiosonde and aircraft**
114 **dropsonde data by Colon.....”**

115
116 2. P.35282, line 15, support product availability at 100 pressure levels looks too high a vertical
117 resolution.

118 **Reply: We once again checked the data product and confirm that we have written correctly. Note that**
119 **we are using support products which are available at 100 pressure levels up to 70 km (0.016mb), but**
120 **we restrict the data from surface to 600 hPa only.**

121
122 3. p.35284, line13-15: MI lies between 900 & 800 hPa. Authors infer MI from DT between 950 and
123 850 hPa. This may be alright for the WAS however, may miss the MI over the EAS. As authors
124 pointed out referring to Colon (1964), MI rises from west to east over the Arabian Sea. So why not
125 define DT between 950 hPa and a level at or above 800 hPa?

126 **Reply: We have examined each and every individual profile to capture inversion height, depth and**
127 **strength. On the basis of this computation, Fig 3 has been generated. From this figure it could be**
128 **ascertained that in more than 95 % of cases, the inversion over Arabian sea is lying in the region 950**
129 **and 850 hPa. Over EAS, It can be seen that the MI lies below 2 km (~ 800 hPa Fig. 3a,b).**

130
131 **We have also mentioned in the text (Page 35285, lines 24 – 25) that “This level criteria (950 –**
132 **850 hPa) was arrived at after a detailed examination of ΔT at a few more level intervals (viz 1000 –**
133 **900 hPa, 1000 – 850 hPa, 850 – 750 hPa etc)”. As mentioned in the manuscript, the upper / lower**
134 **levels of inversion vary on individual days in a small amount (~ 25 hPa). Even if the lower or upper**
135 **level of inversion were at levels above 850 or below 950 hPa by this small amount, the inversions**
136 **would still be captured in the overall ΔT , though of a slightly lesser magnitude.**

137
138 4. Fig. 2, x-axis: Julian day can be used

139 **Reply: We have changed x-axis to Julian day in all the 3 figures.**

140
141 Finally, ERA-interim data might have utilized IASI data product. So, can that be an independent
142 source for comparison?

143 **Reply: As mentioned in the manuscript there is no ground truth (after 1979) over the Arabian sea to**
144 **compare with our results. Hence we have compared with ERA, the only available standard option of**
145 **comparison over AS. We have mentioned the referee's point in the text (Page 35294, lines 5 - 6).**

146
147 There are some grammatical errors and the text can be reduced by eliminating some repetitions.

148 **Reply: We have gone through the text again and tried to eliminate repetitions and grammatical errors**
149 **to the maximum possible extent.**

150

151 Some corrections which we have noticed (now corrected in the text):

152

153 1. One mistake in referring figure on Page 35286 line 23.

154 In text, [Fig.2](#) is replaced with [Fig.3](#)

155

156 2. Page 35282, line 7 Fourier to replace with fourier

157 **Reply: Since Fourier is the name of the scientist we retained it with capital letter F.**

158

159

---END---

160

161

162

163

164

165

166

167

168

169 **Characteristics of Monsoon Inversions over Arabian Sea observed by Satellite Sounder and**
170 **Reanalysis data sets**

171

172 Sanjeev Dwivedi¹, M. S. Narayanan¹, M. Venkat Ratnam^{2*} and D. Narayana Rao¹

173

174 ¹Department of Physics, SRM University, Kattankulathur, Chennai - 603 203, India.

175 ²National Atmospheric Research Laboratory (NARL), Gadanki, Tirupati- 517 502, India.

176

177 * yratnam@narl.gov.in ; Phone: +91-8585-272123; Fax: +91-8585-272018

178

179

180

181 **Abstract**

182 Monsoon inversions (MIs) over Arabian Sea (AS) are an important characteristic associated
183 with the monsoon activity over Indian region during summer monsoon season. In the present study,
184 we have used five years (2009 - 2013) data of temperature and water vapor profiles obtained from
185 satellite sounder instrument, Infrared Atmospheric Sounding Interferometer (IASI) onboard MetOp
186 satellite, besides ERA - Interim data, to study their characteristics. The lower atmospheric data over
187 the AS have been examined first to identify the areas where monsoon inversions are predominant
188 and occur with higher strength. Based on this information, a detailed study has been made to
189 investigate their characteristics separately in eastern AS (EAS) and western AS (WAS) to examine
190 their contrasting features. The initiation and dissipation times of MI, their percentage occurrence,
191 strength etc., has been examined using the huge data base. The relation with monsoon activity
192 (rainfall) over Indian region during normal and poor monsoon years is also studied. WAS ΔT values
193 are ~ 2 K less than those over the EAS, ΔT being temperature difference between 950 and 850 hPa.
194 A much larger contrast between WAS and EAS in ΔT is noticed in ERA-Interim dataset Vis a Vis
195 those observed by satellites. The possibility of detecting MI from another parameter, Refractivity N,
196 obtained directly from another satellite constellation of GPS RO (COSMIC), has also been
197 examined. MI detected from IASI and Atmospheric InfraRed Sounder (AIRS) sounder onboard
198 NOAA satellite have been compared to see how far the two data sets can be combined to study the
199 MI characteristics. We suggest MI could also be included as one of the semi-permanent features of
200 southwest monsoon along with the presently accepted six parameters.

201

202 *Keywords:* Monsoon inversion, Arabian sea, lower atmospheric temperature, satellite sounders,
203 IASI, ERA

204

205

206 **1. Introduction**

207 The Monsoon Inversion (MI) is one of the criteria providing a stability condition over the
208 western Arabian Sea (AS), extending sometimes through to the west coast of India. The MI controls
209 the mid tropospheric moisture content during the different phases of the monsoon. This shallow layer
210 of low level inversion will act as a barrier in uplifting of the moisture, and could act like a wave –
211 guide for transport of water vapour to the mainland. The fluctuation of the rainfall over the west
212 coast of India is more closely related to changes in monsoon circulation over the AS (Das, 2002).

213 The AS is located at the north head of the Indian Ocean. During the monsoon season, Indian rainfall
214 is fully dependent on the physical processes occurring over AS like SST, Somali Low Level Jet and
215 near by it Arabia desert is there which is putting more effect on MI. Thus, MI has been known to be
216 intimately associated with the activity of the Indian southwest monsoon and have a close link with
217 active and break spells (Narayanan and Rao, 2004).

218 MIs were first detected in 1964 during International Indian Ocean Expedition (IIOE) from
219 ship radiosonde data by Colon (1964) and Ramage (1966). Subsequently from satellite derived
220 temperature and humidity data, this feature was detected by Narayanan and Rao (1981). They
221 detected MI despite the coarse vertical resolution (~ 2 km) of the TIROS – N satellite temperature
222 sounding instruments (Thomas,1980) of 1970 – 80's compared to the vertical extent (about 1 to 1.5
223 km) of the phenomena itself. They used a simple differencing technique by finding the difference,
224 ΔT , of sea skin temperature and 1000 to 850 hPa mean layer temperature (MLT) from the satellite
225 sounding data. By adopting this differencing procedure, they assumed that most of the systematic
226 errors/limitations of retrieval methods and vertical resolution of satellite soundings may be getting
227 significantly minimized. Furthermore, the spatial and temporal nature of MIs is quite large compared
228 to normal boundary layer inversions observed over land and other oceans.

229 Using data of about 150 ship radiosonde and aircraft dropsonde profiles and concurrent
230 TIROS – N satellite sounder data of MONsoon_EXperiment (MONEX) conducted in 1979, they

231 showed that regions with $\Delta T \leq 2$ K in satellite derived atmospheric temperatures are associated with
232 AS MI. Study of these MIs over the western AS was one of the three major objectives of MONEX /
233 FGGE -1979 (WMO, 1976). These are seen to be much stronger (temperature departures from
234 normal profiles in some cases being as high as ~ 6 K in the lower 1 - 2 km height region) in contrast
235 to the inversions observed over land or associated with trade wind inversions ($\sim 1 - 2$ K).

236 MIs are characterized by both a vertical temperature increase in the altitude region from 0.5
237 km (in some cases even from surface) to ~ 2 km and with a sharp fall in relative humidity (RH)
238 above this altitude region. Some of the observed features of MIs reported from the limited
239 observations to date (Colon, 1964; Ramage, 1966; Narayanan and Rao, 1981; 1989) are: (i) strength
240 decreases and base increases as one moves from the west to east AS, (ii) oscillation of its lateral
241 boundary from west to east with the activity of monsoon and (iii) associated oscillation of mid
242 tropospheric water vapor content from east to west, i.e. in the opposite sense to the boundary of
243 temperature inversion. The two primary causes proposed (Colon, 1964) for formation/maintenance
244 of monsoon inversion are: (a) hot air advection from Arabia (~ 700 hPa) riding over cool maritime air
245 (at levels below ~ 800 hPa) from south Indian Ocean and (b) subsidence over western AS associated
246 with monsoon convection over main land. This large scale subsidence had played a major role in the
247 maintenance of MI during the prolonged weak monsoon of 2002 (Narayanan et al., 2004).

248 However, not much attention was paid to the study of MI due to paucity of freely available
249 data over this region. The spatial density of TIROS – N satellite data available to the global, research
250 community in 1979 was just a single temperature – humidity profile a day in a latitude – longitude
251 grid box of $2.5^\circ \times 2.5^\circ$ (Kidder et al., 1995). Narayanan and Rao (1981) had to adopt temporally a
252 pentad and spatially a $5^\circ \times 5^\circ$ average to detect statistically significant results from the meager data
253 available then. Since 2008, the density of temperature and humidity profiles from polar orbiting
254 satellites is nearly two orders of magnitude higher (about one vertical profile every 50×50 km, twice
255 each day and from two satellites) besides with a much better vertical and spectral resolution. Thus, it

256 has become possible now to study MI phenomena in greater detail. However, no in-situ data after the
257 1979 experiment are available in this region.

258 In the present study, we have used the high resolution and better accuracy temperature and
259 humidity profiles data obtained from Infrared Atmospheric Sounding Interferometer (IASI) onboard
260 MetOp satellite. These data have higher vertical resolution, i.e., ~ 400 m below 700 hPa, which is
261 much better than those of TIROS – N of MONEX 1979 period. Further, ERA-Interim data have been
262 used to compare the MI features seen in them with those from the satellite data. For explaining the
263 relative contribution of subsidence and convection on MI, where only wind observations are
264 required, ERA-interim reanalysis data have been used. The temperature - humidity profile data are
265 also available from NOAA – Atmospheric InfraRed Sounder (AIRS) instrument since 2002, all of
266 which have also been analysed in the same way as the IASI data. —However, we have not presented
267 those results here, because of some inconsistencies (i.e. sometimes ERA – interim data shows MI but
268 AIRS has different features like no MI present, profile to profile match between AIRS and ERA-
269 interim datasets are not seen i.e. inversion type changes or level of inversion changes) observed
270 between the IASI and AIRS data in studying the MI features. Thus, we have confined the present
271 study to data only from one instrument, viz., IASI, which had been reported to be performing better
272 (Smith et al., 2015). This is expected to also ensure that the results of temporal and spatial gradients
273 of ΔT presented here (featuring MI) will be mutually consistent – even if the absolute values of
274 temperature/humidity may be having some errors. We have, however, included one section
275 describing the discrepancies between the results of these two instruments for studying the MI
276 features. We have also shown to a limited extent the potential of the GPS RO measured ‘refractivity’
277 profiles in delineating inversion regions. For this we have also used the MONEX in-situ temperature
278 – humidity profiles of 1979.

279 **2. Data**

280 As mentioned earlier, data from a variety of instruments have been used in this study – viz
281 from IASI satellite instrument, ERA-Interim reanalysis data and, in-situ dropsondes/ radiosondes
282 data obtained during MONEX – 1979. Limited AIRS sounder data and GPS RO data have also been
283 presented for comparison purposes. A short description of each of these data are given in the
284 following sub-sections and also summarized in Table 1.

285 **2.1. IASI observations**

286 The IASI instrument (Clerbaux et al., 2007; 2009) measures the profiles of temperature
287 profiles in the troposphere and lower stratosphere with a high accuracy (~1K root mean square) at a
288 vertical resolution of 1 km in the lower troposphere), as well as humidity profiles in the troposphere
289 (10–15% accuracy with a 1–2 km vertical resolution) primarily for numerical weather prediction
290 (Schlüssel et al., 2005). IASI is a thermal infrared nadir-looking Fourier transform spectrometer
291 which measures the Earth’s surface and the atmospheric radiation over a spectral range of 645–2760
292 cm^{-1} with a 0.5 cm^{-1} spectral resolution. The IASI field of view is a matrix of $2^\circ \times 2^\circ$ circular pixels,
293 each with a diameter footprint of 12 km at nadir. It measures on an average at each location on the
294 Earth’s surface twice a day (at 09:30 and 21:30 hr local time), every 50 km at nadir, with an
295 excellent horizontal coverage due to its polar orbit and its capability to scan across track over a swath
296 width of 2200 km. More details about retrieval and validation are presented in Kwon et al. (2012).
297 The support products, which we have used, are available at 100 pressure levels at 50 x 50 km
298 horizontal grid spacing. but we restrict the data from surface up to 600 hPa only.

299 **2.2. Dropsonde / Radiosonde measurements MONEX (1979)**

300 For the in-situ ground truth comparisons over AS between the longitudes 55° - 75° E we also
301 make use of the aircraft dropsondes and ship radiosonde observations obtained during MONEX
302 1979. MONEX was conducted during May - July 1979 and there were 416 radiosondes and 412
303 dropsondes measurements over AS. It may be noted that after the MONEX campaign in 1979, no
304 campaign has been organized to get in-situ data over western or central AS. During the Indian

305 ARMEX programme (2002), however, some in-situ data were available but only in the far eastern
306 AS (east of 70°) near the coast of India. Table 2 summarizes the comparison of in-situ observations
307 with satellite data of 1979 by Narayanan and Rao (1981). This information on ΔT criterion has been
308 used as the basis in the present study.

309 **2.3. ERA-Interim data**

310 The European Centre for Medium Range Weather Forecasts (ECMWF)-Interim is one of
311 most advanced in operational use for diagnosing the global atmosphere with an accuracy that is less
312 than what is theoretically possible (Simmons and Hollingsworth, 2002; Simmons et al., 2007). The
313 selected variables are specific humidity along with the temperature on different pressure levels. The
314 atmospheric data are available at $0.125^\circ \times 0.125^\circ$ latitude and longitude grids on 37 pressure levels
315 from 1000 to 1 hPa; however, we have used data of 14 pressure levels from 1000 to 600 hPa for the
316 period of 2009 to 2013 for the present study. Vertical as well as horizontal strength of MI have been
317 examined from these data sets and compared with satellite observations.

318 **2.4. AIRS observations**

319 AIRS onboard the Earth Observing System (EOS) - Aqua satellite of NASA was launched in
320 2002. This is also a polar orbiting satellite which crosses the equatorial latitudes at 13:30 hr LT and
321 01:30 hr LT for the ascending and descending pass, respectively. The orbit period is 98.99 min, and
322 the orbit is sun synchronous with consecutive orbits separated by 2760 km at the equator. AIRS has a
323 field of view of 1.1° and provides a nominal spatial resolution of 13.5 km for IR channels and
324 approximately 2.3 km for visible/near-IR channels. AIRS data together with data from the Advanced
325 Microwave Sounder Unit (AMSU) (Lambrigtsen, 2003) are used in the present study. We make use
326 of AIRS support data which have higher vertical resolution with 100 levels between 1100 and 0.016
327 hPa. For the present study we restrict data only from surface to 600 hPa which have vertical
328 resolution of 30-20 hPa. Though these data are available since 2003, we make use data from 2009
329 only so as to compare with other data sets.

330 **2.5.COSMIC GPS RO**

331 GPS RO technique is also a remote sounding satellite technique, and it uses the radio signals
332 received onboard a low Earth orbiting satellite from atmospheric limb sounding. The GPS RO
333 measurements have a vertical resolution ranging from 400 m to 1.4 km, which is much better than
334 that of any other satellite data (Kursinski et al., 1997). COSMIC has vertical resolution of ~ 100 m in
335 the lower troposphere for temperature. The COSMIC GPS RO was successfully launched in mid-
336 April 2006 (Anthes et al., 2008). Since 17 July 2006, COSMIC GPS RO provides accurate and high
337 vertical resolution profiles of atmospheric parameters that are almost uniformly distributed over the
338 globe. COSMIC provides a direct estimate of refractivity (from measurement of bending angle by
339 GPS technique) at very high vertical resolution, but have poor repetivity.

340 **3. Methodology and analysis procedure**

341 As mentioned earlier, MI was first observed by Colon (1964) and Ramage (1966) over the
342 AS from ship upsonde profiles. They reported that MI lies between 900 and 800 hPa with strong
343 intensity over western AS (WAS) and weakens as its base rises and comes to eastern AS (EAS).
344 Following this study, Narayanan and Rao (1981) have shown MI's presence using the temperature
345 difference (ΔT) between the TIROS-N derived sea skin temperature and atmospheric layer mean
346 temperature (between 1000 hPa and 850 hPa).

347 Note that lapse rate (dT / dz) of atmosphere at the tropospheric altitudes is a negative
348 quantity. However, in this study (and also of Narayanan and Rao, 1981), we have considered ΔT as
349 temperature difference between a lower level (higher temperature) and a higher level (lower
350 temperature), so is normally a positive quantity of value ~ + 6 to + 7 K. For inversion regions, it is
351 negative or a small positive quantity (i.e. less than + 2 K).

352 After considering several limitations in the satellite data of that time, Narayanan and Rao
353 (1981) finally considered MI when the difference ΔT , between surface and layer mean temperature
354 (of 1000 to 850 hPa), is 2 K or less, which otherwise was greater than 3 K. Since then, several

355 improvements in the satellite instruments, retrieval techniques and data products have come up in
356 these three decades.

357 Extensive in-situ observations of AS MI features were obtained during FGGE-MONEX 1979
358 experiment. Fig. 1a shows a typical example of MI observed in T (temperature) and RH (Relative
359 Humidity) data obtained on 27 June 1979 at 0656 GMT at 20°N, 62°E from radiosonde. In this
360 example MI starts from surface and temperature departure is as high as ~ 10 K from a normal lapse
361 rate profile at 900 hPa. The vertical extent of inversion varies from 0.5 km to even more than 1 km.
362 It is to be noted that AS MI are much stronger and long lasting i.e. less diurnal variation than normal
363 boundary layer and persist for many days compared to those over land regions.

364 A detailed analysis is made in this study by considering several thousands of profiles
365 obtained from different satellite observations now available over AS for redefining MI. Since the
366 MIs occur at low levels, first we tried with the earlier adopted criteria of Narayanan and Rao (1981)
367 i.e., by taking difference between sea surface (skin) temperature and 925 hPa level (mean pressure
368 level of 1000 - 850 hPa MLT of TIROS-N data of the 1980 time frame) temperature and found those
369 to be noisy for detecting MI. To avoid the surface emissivity effects in the retrieval at / near surface
370 (from the sounder instrument), we adopted the lower level in the present study as 950 hPa instead of
371 sea surface / skin temperature. It was considered not appropriate to use SST/skin temperature
372 (though may be of higher accuracy) from a different source (viz imager onboard the same satellite)
373 for estimating ΔT . It was felt that this will not give the advantage of the differencing procedure
374 employed earlier to detect inversion (Narayanan and Rao, 1981). This level criterion (950 – 850 hPa)
375 was arrived at after a detailed examination of ΔT at a few more level intervals (viz 1000 – 900 hPa,
376 1000 – 850 hPa, etc).

377 Thus, we have used:

$$378 \quad \Delta T = T(950 \text{ hPa}) - T(850 \text{ hPa}) \quad (1)$$

379 to delineate MI. However, the actual levels used were 958 hPa and 852 hPa at which the support data
380 are available from the NOAA website.

381 While considering the normal atmospheric lapse rate of + 6 to +7 K / km (average of 340
382 non-inversion cases obtained during MONEX, figure not shown), it is expected to observe a ΔT of +
383 6 to +7 K between 950 and 850 hPa (~ 1 km height difference). Note that Narayanan and Rao (1981)
384 have identified inversion (non-inversion) region as $\Delta T \leq + 2$ K ($\Delta T > + 2$ K) in TIROS – N satellite
385 data for a height range difference of ~ 0.75 km. For the present study (for 1 km height difference) the
386 same would translate to $\Delta T \sim + 2.7$ K for inversion delineation. However, to be on the safe side and
387 to provide margin of error, we have still considered $\Delta T \leq +2$ K as criterion of inversion region. The
388 interval 2.0 K to 2.7 K may still be a grey region which could be interpreted as inversion region on
389 some occasions. The criterion of $\Delta T \geq + 4$ K as non – inversion regions has been adopted. In the
390 example shown in Fig. 1a, ΔT is (minus) - 1.3 K (note however, that the actual inversion value is ~ -
391 5 K between surface and 900 hPa).

392 In general, a sudden drop in the water vapor just above the inversion is observed (e.g. RH
393 drop of ~ 70% in Fig 1a). Since all the data sources mentioned in section 2 provide water vapor
394 information, we also have examined the changes happening in water vapor near/above the inversion
395 altitude. In general, inversion is identified in the temperature (water vapor) where it increases
396 (decreases sharply) instead of decreasing (decreasing gradually) with altitude. For obtaining detailed
397 characteristics of MIs over the Arabian sea, we have selected three $3^\circ \times 3^\circ$ grid boxes centered at
398 latitude 18.5° N, and located at longitudes 60° E as WAS, 64° E as CAS (central AS), 71° E as EAS
399 (as shown in Fig. [32](#)).

400 **3.1. Quality checks for the profiles and volume of data**

401 Each temperature profile from the satellite data was interpolated from surface to 500 hPa (26
402 levels of support data) at 0.25 km intervals for our preliminary analysis. We have used the quality
403 flag 0 and 1 from the given data set which are corresponding to best and good. There were many

404 erroneous profiles which could be observed even from a cursory examination of the data. The
405 temperatures at a few / more levels were far wide of the normal profile. To account for these types of
406 profiles, we applied a quality check to filter out spurious data. All profiles of July and August
407 months of 2009 (poor monsoon year) and 2011 (normal monsoon year) were sorted out in 3 x 3
408 boxes of WAS and EAS. -For each month the mean and standard deviation were obtained for each
409 interpolated levels separately. Those profiles for which the data at any one level was lying beyond +/
410 - 2 sigma of the mean, were not considered for further analysis. From this procedure we saw that
411 nearly 25 – 30 % of profiles were getting filtered out.

412 Using these quality checked profiles, the procedure for selecting the right levels for
413 calculating ΔT was established. Thereafter, for all the other monsoon days of the five years, we have
414 computed ΔT for individual profiles by an automated procedure (without resorting to examining each
415 profile). They were grouped and their ΔT values averaged in $1^\circ \times 1^\circ$ bins over the whole AS region.
416 Diurnal variation of ΔT was examined for a few months of data. -Once we made sure that this is not
417 discernible, the day and night data of a calendar day were merged in $1^\circ \times 1^\circ$ boxes.

418 For further analysis, the average ΔT values for the day (24 hr period) at $1^\circ \times 1^\circ$ grids have
419 been used. Due to averaging of ΔT of all the profiles in $1^\circ \times 1^\circ$ box and morning and evening passes
420 (~ 6 to 8 values of ΔT in 24 hours), the strength of MI may be getting somewhat reduced (as MI
421 occur at slightly different levels within a vertical range of 25 - 50 hPa, for different profiles in the
422 same $1^\circ \times 1^\circ$ box). For some studies (e.g. for Fig 2, 4, 5, etc), we have used only a limited data from
423 this total data set. The total number of profiles considered for the five years amount to nearly half a
424 million, each for AIRS and IASI – considering that nearly 30 % profiles did not pass through our
425 quality check.

426 **4. Results and Discussions**

427 **4. 1. Monsoon Inversions observed in satellite and ERA-Interim datasets**

428 Fig. 1a and 1b show MI observed on 27 June 1979 at 0730 GMT at 20°N, 60°E through
429 MONEX radiosonde and ERA – Interim data, respectively. The detailed comparison study between
430 TIROS – N satellite data of 1979 and concurrent in-situ MONEX radiosonde profiles for 1979
431 southwest monsoon carried out by Narayanan and Rao (1981) is summarized in Table 2. This was
432 the only occasion (1979) when in-situ data were available over AS to compare with satellite
433 soundings. Thus, comparison of current satellite observations is being done in this study with ERA-
434 Interim data. In this case, ERA – Interim data also catches the inversion but with a less rise in
435 temperature (~ 3 - 4 K) and decrease in RH (~ 60%). To show how the present day satellites reveal
436 MI, typical profiles of temperature and RH obtained from collocated IASI and ERA-Interim on 30
437 July 2009, 0530 GMT are plotted in Fig. 1c, and 1d, respectively. A clear MI in the satellite profile
438 and ERA-Interim can be noticed though with somewhat varying strengths and base of inversion
439 height. However, the top height of inversion is consistent. These are the first reported results of MI
440 features seen directly from the satellite observations over the AS which were shown earlier by
441 Narayanan and Rao (1981) in an indirect way by using ΔT indices. In general, in the individual
442 satellite profiles, we are able to see the MI strengths ranging from ~ + 2 to - 6 K (-8.8 K being the
443 actual temperature difference between 930 hPa and 850 hPa in Fig. 1c). These MI lie mostly below
444 850 hPa level, but in rare occasions we could see them even up to 700 hPa over the EAS – but of
445 much weaker strength. The strength of MI is also seen to be decreasing from WAS to EAS which
446 will be discussed in detail in later sections.

447 Thus, in Fig. 1, we have seen examples of MI comparison between radiosonde and ERA
448 interim (1979) and between IASI and ERA-Interim (2009). There are some minor inconsistencies by
449 way of inversion heights in individual profiles of the three data sets. However, our objective here is
450 to examine the large scale characteristics of MI by considering average ΔT computed from individual
451 profiles in 1° x 1° grids.

452 **4. 2. Contrasting behavior of MI between WAS and EAS**

453 As observed from Fig. 1, MI can lie between surface and ~ 2 km during Indian Summer
454 Monsoon (ISM) season (JJAS). Careful examination of time evolution of ΔT over the western
455 Arabian sea reveals that the MI start forming around first half of May and dissipate around late
456 September. Fig. 2 shows the evolution of the MI during two contrasting years (2009 a poor monsoon
457 year and 2011 a normal monsoon year). During the peak monsoon season of July – August, the
458 difference in ΔT between the two years are prominently noticed. Also MI is more frequently
459 observed with higher strength during the peak monsoon months of July and August. To investigate
460 further their contrasting features in WAS and EAS, data only of July and August from 2009 to 2013
461 are presented.

462 In Fig. 3 we have summarized the three important characteristics of MI viz their base altitude,
463 strength (as revealed by ΔT) and percentage occurrence during the complete season. For brevity, the
464 results of only July and August months, averaged for all the five years 2009 – 2013 are shown in the
465 figures. Fig. 3a and 3b show the spatial variation of base altitude of MI during July and August,
466 respectively. The contrasting feature of base altitude of occurrence of MI is seen mainly north of 15°
467 N from the selected three grid boxes. It increases from WAS (below 1 km) to EAS (above 1.5 km)
468 through CAS (1.0 -1.5 km).

469 As mentioned earlier, from very limited observations previous studies (Colon, 1964; Ramage,
470 1966; Narayanan and Rao, 2004) had suggested that strength and frequency of occurrence of the MI
471 will be more over WAS than over EAS. To investigate this contrasting behavior of MI in detail from
472 satellite soundings, we examined the spatial variations of ΔT . Fig. 3c (July) and 3d (August) shows
473 the strength of MI increasing from EAS to the WAS and is prevalent mainly north of 15°N latitude
474 extending from 15°N to 25° N latitude and 55° E to 68° E longitude. The strength of MI can be
475 noticed as ~ + 2 K near Arabia coast and as we approach Indian coast, the normal environmental
476 lapse rate condition of + 6 to + 7 K/km are encountered. From these figures a clear contrast in ΔT a
477 difference of around 2 K in the southeast quadrant of AS between July and August is also noticed. In

478 general, the AS is covered with lapse rate of + 4 K/km, which is the condition for taking the
479 atmosphere towards stability during the August month. The region of Somali low level jet is the
480 location of permanent region of MI during the month of July. In the spatial distribution of monsoon
481 low level jet shown by Roja Raman et al. (2011) reveals that the center of the core is seen around
482 13°N and 60°E and exists strong shear between 850 hpa and 700 hpa. Strong surface winds of south-
483 west monsoon produce an Ekman transport perpendicular to the wind flow with strong upwelling in
484 the region which in turn brings the cool water from the deeper layers to surface. Simon et al. (2007)
485 showed that WAS region is the region of Somali upwelling, and also since the low level jet and
486 surface wind are of the order of ~ 20 m/s, they produce sufficient cooling and the air above this
487 region is still warmer when compared to the upwelling area, producing strong inversion.

488 Fig. 3e and 3f shows the spatial variation of percentage occurrence (PO) of MI during July
489 and August months. PO is calculated corresponding to $\Delta T \leq + 2$ K criteria. In general, it is observed
490 that WAS show more number of MI cases (50 to 70%) compared to EAS (10 to 20%). ERA-Interim
491 data show only 30 to 50% cases of MI over WAS which will be dealt in detail in the following sub-
492 sections. The maximum PO during the four months of monsoon over the WAS are 40 % (June), 60
493 % (July), 50 % (August) and 30 % (September) (figure not shown). The areal extent of the maximum
494 PO is seen during July. During September, very small area of Northern AS is covered with ~ 50 %.
495 No inversion is seen in the EAS box during the June and September periods. Despite its low strength
496 (ΔT) PO show maximum occurrence of 60% in July. Since the PO and strength of MI over the CAS
497 is in between the features of EAS and WAS, for further discussions pertain, only WAS and EAS
498 boxes.

499 The PO of ΔT value in different ranges observed in IASI for the five monsoon seasons is
500 shown in Fig. 4. ΔT values range from -2 to + 6 K (0 to + 7 K) in WAS (EAS) with peak occurring
501 around + 1 to + 2 K (+3 to +4 K). There are only a few values of ΔT less than + 2 K in EAS. Similar
502 analysis is also made using ERA-Interim data and is shown in bottom panels of Fig. 4. ERA-Interim

Formatted: Superscript

Formatted: Superscript

503 data shows the contrast between WAS and EAS more clearly. In case of q at 700 hPa a difference of
504 about 2 g/kg can be noticed, with EAS having higher humidity values than WAS in IASI. However,
505 ERA-Interim data does not show this distinction.

506 To further examine the contrasting behavior between EAS and WAS, time series of ΔT and
507 water vapour at 700 hPa is considered for different years. Daily mean variations of ΔT and specific
508 humidity, q , at 700 hPa in WAS and EAS during the monsoon season of the year 2012 observed by
509 IASI is shown in Fig. 5. Note that we have included results of all the days irrespective of whether MI
510 is present or not. Three point average smoothed curves are shown in the respective panels. In
511 general, it can be seen that WAS ΔT (q at 700 hPa) values are $\sim + 2$ K (1 - 2 g/kg) less than those
512 over EAS for the season as a whole (Fig. 5a and 5b). During all the years (2009 - 2013) of the
513 present study, IASI reveals (figure not shown) this feature. Similar analysis has been carried out
514 using ERA-Interim reanalysis data and is shown in Fig. 5c and 5d. A clear contrast between WAS
515 and EAS in ΔT can be noticed in ERA-Interim data. A mean difference of ~ 2 K (~ 1 g/kg) can be
516 noticed in ΔT (q at 700 hPa) between WAS and EAS, EAS values being lower. A cyclic behavior in
517 ΔT variations with a period of ~ 20 -25 days in case of ERA-Interim is noticed but not observed in
518 the satellite measurements. There exists no significant diurnal variation in ΔT (figure not shown).
519 This was verified before averaging ΔT of all profiles (day and night) in the $1^\circ \times 1^\circ$ grids. Due to
520 inversion and stability, moisture is getting trapped at lower levels over WAS compared to EAS as
521 indicated in Fig. 5b and 5d observed from IASI and ERA-Interim, respectively.

522 **4.3. Relation between MI over AS and monsoon activity**

523 Past investigations (e.g. Gadgil and Joseph, 2003) showed that the mesoscale monsoon
524 features largely vary with the activity of the monsoon. In general during the active phase of the ISM,
525 typically there will be more precipitation over central India (18° - 28° N and 65° to 88° E). Similar
526 variations in precipitation during the monsoon season can also be expected on regional scales.
527 Gadgil and Joseph (2003), Kripalani et al. (2004), Rajeevan et al. (2006) have considered the daily

528 rainfall time series over central India during monsoon months along with the climate normal to
529 delineate 'active' and 'break' periods over the Indian region. On the basis of this data, Rajeevan and
530 Bhate (2009) have defined active and break phases over central India by considering the days
531 exceeding the climate mean with +1 (-1) standardized anomaly as active (break) periods provided it
532 should persist at least for 3 days (triad).

533 Fig. 6 shows the latitude - longitude cross section of ΔT and q at 700 hPa for active (14 - 17
534 July 2009) and break (30 July - 11 Aug. 2009) spells for the monsoon season of 2009 observed using
535 IASI and ERA-Interim data. Irrespective of the data source, ΔT and associated q at 700 hPa reveal
536 that a large part of WAS is covered with MI ($\Delta T \leq +2$ K and less moisture values) up to west of \sim
537 68° E during the break spell as seen in Fig. 6a and 6e. In the north AS, MI reach as close as Gujarat
538 coast during break spells (especially in ERA-Interim data), but are restricted to WAS during active
539 spells. During the active spell, the inversion regions from ΔT maps are patchy west of 65° E in Fig.
540 6c. Also strengths of ΔT in WAS are more as observed by ERA-Interim than by IASI during break
541 spells. ERA-Interim shows (Fig. 6e and 6g) more smoothed results and there is less change in area
542 extent in this case. Specific humidity q at 700 hPa shows clear result that during the break spell AS
543 has less moisture and more during the active spell. One can notice the feature of inversion from the
544 figure where water vapor is being trapped in the lower portion resulting in less moisture over WAS
545 and more over the EAS. Thus, the q values also give a good indication of the inversion feature.

546 **4.4. MI during normal and poor monsoon years**

547 It is well known that strong MI suppresses the vertical development of clouds; rain cannot
548 occur in such situations (Sathiyamoorthy et al., 2013). Using ARMEX-I (2002) data, Bhat (2006)
549 could notice strong and persistent inversions in the atmosphere over the AS and west coast of India.
550 This data proved very valuable as July 2002 rainfall was the lowest in the recorded history and the
551 data collected over the AS and on the west coast helped in understanding the conditions that
552 prevailed over the eastern AS during one of the worst monsoon years. The relation between MI and

553 central India rainfall is further investigated by separating the MI observed during normal (2010 -
554 2013) and poor monsoon (2009) years. Time variations of ΔT observed over WAS during two
555 contrasting years of 2009 and 2011 obtained from IASI measurements and ERA-Interim data are
556 shown in Fig. 7. It can be seen that good monsoon year 2011 has higher ΔT than poor monsoon year
557 2009 (Fig. 7a), and is the same for q i.e. higher value for the year 2011 (Fig. 7b). ΔT is observed to
558 be lower by about 2 K during the season as a whole in the poor monsoon year when compared to the
559 good monsoon year, suggesting the possibility of a variation of this parameter between normal and
560 poor monsoon years. This aspect is clear from the right panels where difference between 2011 and
561 2009 observed in ΔT (Fig. 7c) and q at 700 hPa (Fig. 7d) are shown. From this figure we can infer
562 that the year 2009 has less value of ΔT and less value for q suggesting stronger MI during poor
563 monsoon year. Note that during most of the time, the temperature in 2011 is higher (the difference
564 between 2011 and 2009 showing positive values) and less temperature lapse rate means more stable
565 layered atmosphere. In 2011, WAS temperature show higher values revealing less MI over AS when
566 compared to 2009. The decreasing trend in ΔT is discernible in difference plots for some particular
567 epochs. In general, ERA-Interim also show these features (Fig. 7e and 7f), but only to a moderate
568 extent. It may be noted that these inferences are based on the results of only one poor monsoon year
569 (2009).

570 **4.5. Inter-comparison of MI features with IASI, AIRS and ERA**

571 Inter-comparison of the gross features of PO of MI (with $\Delta T \leq 2$ K) in WAS and EAS
572 | estimated for the ~~five~~ years of monsoon season by IASI, ~~and~~ AIRS and ERA-Interim data are
573 | shown in Fig. 8. In general, when we consider ΔT as a parameter to detect MI, clear contrasting
574 | feature between WAS and EAS with higher PO in WAS can be noticed in all the data sources
575 | mentioned above. PO in the IASI measurements ranges from 23% to 54%. Among these data sets,
576 | ERA-Interim shows huge difference in the percentage occurrences between WAS and EAS, to the
577 | extent that not even a single MI is ~~sometimes~~ seen in EAS in any year. Since the vertical resolution

578 of the IASI temperature profiles is better than ~~even~~AIRS, higher PO of MI in the WAS is noticed
579 throughout when compared to AIRS, except in the case of 2012. However, ERA- Interim being a
580 combination of model and observations, it is not able to pick up the MI in the EAS where the
581 strength of inversion is also weak. The artifact of the model appears to be smoothening the MI
582 features of IASI when it is assimilated in the ERA – Interim.

583 Coming to the satellite observations, during five years, IASI shows higher PO of MI than
584 AIRS except for 2012 for WAS. ~~When we consider EAS as a place to detect MI, AIRS observed~~
585 ~~always higher PO than IASI and almost nothing is noticed in ERA-Interim.~~ A distinct contrast
586 between WAS and EAS with higher PO in the former region can be noticed. When we consider EAS
587 as a place to detect MI, AIRS observed always higher PO than IASI and almost nothing is noticed in
588 ERA-Interim. Thus, we may infer that IASI is performing better than AIRS for detecting MI (as
589 ERA is in better agreement with IASI rather than with AIRS). ~~Thus, it can be concluded that IASI~~
590 ~~performs better than AIRS in detecting MI.~~ Note that large inter-annual variability in MI is observed
591 and this is expected to reflect in the monsoonal activity over Indian region. It can also be seen that
592 there is a steady decrease of PO of MI as observed by IASI from 2009 to 2013. No such feature is
593 observed in AIRS – which shows more random behavior over the different years.

594 We have made the scatter plot of ΔT observed by IASI and AIRS over WAS and EAS (figure
595 not shown). The scatter does not suggest that these two data sets can be combined to study the small
596 changes of ΔT in their intra-seasonal and inter-annual variations. This and the other differences
597 related to q at 700 hPa constrained us not to combine the AIRS data with IASI data in the present
598 study.

599 **4.6. Monsoon Inversion derived from other parameters**

600 Narayanan and Rao (1989) had also considered equivalent potential temperature (θ_e)
601 differences to study MI. θ_e incorporates the effect of both temperature and humidity. However, the
602 dynamic range of $\Delta\theta_e$ is no better than that of ΔT . Recall that the troposphere is statically stable on

603 | average, with a potential temperature gradient of 3.3 K/km (Wallace et. al., 2006). We make use of
604 | another index here viz atmospheric refractivity (N) for identifying MI. Similar to θ_e , Refractivity
605 | (N), is another atmospheric parameter which is a function of temperature and water vapor. It was
606 | shown that better information on boundary layer can be obtained from refractivity profiles than
607 | virtual potential temperature though both has temperature and water vapor information (Basha and
608 | Ratnam, 2009). Refractivity, N has a higher dynamic range and vertical variation as compared to
609 | temperature (~ 15 N units vis a vis 2 K). More advantage of using N for delineating MI will be
610 | available, provided, it is measured directly, for example, using GPS Radio Occultation technique,
611 | instead of computing it from temperature and water vapor obtained from the sounders or from
612 | radiosonde. However, the spatio-temporal density of direct N observations is too sparse to get
613 | meaningful statistics over equatorial regions.

614 | We have computed refractivity N, from temperature and water vapor data of IASI (and
615 | MONEX radiosonde data), given by the expression:

$$616 \quad N = 77.6 \left(\frac{P}{T} \right) + 3.73 \times 10^5 \left(\frac{e}{T^2} \right) \quad (2)$$

617 | Where P is pressure, T temperature and e water vapor pressure.

618 | Similar to ΔT we have defined an index ' ΔN ' as:

$$619 \quad \Delta N = N(950 \text{ hPa}) - N(850 \text{ hPa}) \quad (3)$$

620 | Profile of N computed from the temperature and humidity profiles of dropsonde (Fig. 9a) of
621 | MONEX time is shown in Fig. 9b. A drastic decrease in N (by 129 N units between 950 and 850
622 | hPa) can be noticed near MI altitudes in this example. Thus, N can also be taken as a potential
623 | parameter to delineate inversion and for studying spatial and temporal variations of MI.

624 | In order to see the relation between ΔT and ΔN , we have estimated ΔN using all the MONEX
625 | profiles obtained over AS. These include both inversion and non-inversion cases. There were 32
626 | (346) profiles with inversion (non- inversion). Note that $\Delta T \leq + 2$ K and $\Delta T > + 4$ K are only

627 considered for obtaining above statistics and there exists 34 profiles in the transition zone (+ 2 to + 3
628 K). Scatter plot between ΔT and ΔN for all 411 in-situ profiles of MONEX over AS is shown in Fig.
629 9c. Correlation coefficients between the two parameters are found to be 0.56 with 15.7 as standard
630 deviation. Note that $\Delta T \leq + 2$ K (inversion region) corresponds to $\Delta N > 50$ N units which is shown
631 as blue line in Fig. 9c. We can infer that if ΔN is less than 50 N units it corresponds to non-inversion
632 region (ΔN more than 50 may be inversion or otherwise). ΔN is thus a supportive parameter to ΔT in
633 identifying inversion / non inversion. Because of its larger dynamic range, details of inversion have
634 been identified in the ΔT and ΔN maps (figure not shown).

635 It is well known that COSMIC satellites are able to provide N profiles directly. The spatial
636 and temporal sampling of COSMIC at any particular region are, however, very meager. The
637 comparison map of ΔN from IASI and ΔN from COSMIC combined for a long break spell from 30
638 July to 11 August 2009 has been studied. This long period accumulation of data was necessary to
639 have sufficient data points from COSMIC to cover the entire AS. One can see ΔN values above 50 N
640 units (inversion region) covering the entire Arabian sea corresponding to ΔT values being below 2 K
641 (shown by IASI, figure not shown). Over the AS region ΔN observed for all the five years of our
642 study was combined to produce the frequency distribution of ΔN over Western AS (5 – 25 °N, 56 –
643 65 °E, excluding land) and Eastern AS (5 – 25 °N, 66 – 75 °E, excluding land) and is shown in Fig
644 10. Over WAS, 712 cases and over EAS 547 cases are showing $\Delta N > 50$ N units (which may be
645 supportive to inversion). A difference of about 10 N units can be noticed, with WAS having higher
646 ΔN values.

647 **5. Summary and Conclusions**

648 Low level MI characteristics, which usually occur below 700 hPa over the AS during
649 southwest monsoon months, have been identified directly from operational satellite temperature
650 retrievals. For the first time we have shown here cases of direct and unambiguous delineation of MI
651 from the satellite temperature and water vapor retrieval observations. We have used five years (2009-

652 2013) data of two different satellite sounder instruments (mainly from IASI and for inter comparison
653 AIRS) along with ERA-Interim reanalysis data to delineate the characteristics of MI over AS. Their
654 percentage occurrence, base height and strength have been studied. For supporting our findings, we
655 also compare with the campaign of MONEX 1979 in-situ measurements over AS. The main findings
656 obtained from the observational study are summarized in the following:

- 657 1. Percentage occurrences of MI over WAS (up to $\sim 65^{\circ}\text{E}$) is $\sim 60 - 70\%$ and are always higher
658 and stronger than over EAS. WAS ΔT values are $\sim 2\text{ K}$ less than those over EAS.
- 659 2. MI is stronger during poor monsoon year (2009) and occurs on more occasions in WAS
660 during break spells. Whether this is true or not for all poor monsoon years need to be checked
661 with more years of data.
- 662 3. ERA-Interim is also able to provide these features but is restricted to some parts of AS with
663 more smoothed variability.
- 664 4. Inter-comparison of IASI and AIRS profiles from the view of study of inversion suggests the
665 differences do not warrant a mix of these two data sets for this study.
- 666 5. The refractivity data has only a supporting role to identify monsoon inversion regions.

667 Thus, MI seems to be a semi-permanent feature of Indian summer monsoon. It is suggested to
668 include this feature also in future monsoon diagnostic and forecast studies.

669

670 **Acknowledgments:** This work is a part of the INSAT – 3D project sponsored by the Indian Space
671 Research Organization (ISRO), for which we are thankful to Space Applications Centre,
672 Ahmadabad. We wish to thank C. M. Kishtawal, V. Sathiyamoorthy, S. GhouseBasha, Jyotirmayee
673 and Ranjit Thapa for discussions and for help in data processing aspects and help in using HPCC.
674 The authors would like to thank ECMWF (<http://apps.ecmwf.int/datasets>) for providing data of ERA-
675 Interim, GESDISC(<http://mirador.gsfc.nasa.gov/>forAIRS)for AIRS, NOAA

676 (<http://www.nsof.class.noaa.gov/>for IASI) for IASI through ftp. We also thank IMD for providing
677 rainfall data over Indian land mass.

678 **References**

- 679 Anthes, R. A., et al.: The COSMIC/FORMOSAT-3 mission: Early results, *Bul. Am. Meteor. Soc.*,
680 89, 1–21, 2008.
- 681 Basha, G. and Ratnam, M. V.: Identification of atmospheric boundary layer height over a
682 tropical station using high-resolution radiosonde refractivity profiles: Comparison with GPS radio
683 occultation measurements, *J. Geophys. Res.*, 114, D16101, doi:10.1029/2008JD011692, 2009.
- 684 Bhat, G. S.: The Indian drought of 2002: a sub-seasonal phenomenon, *Q. J. Roy. Meteor. Soc.*, 32,
685 2583-2602, 2006.
- 686 Clerbaux, C., et al.: The IASI/MetOp mission: First observations and highlights of its potential
687 contribution to GMES, *COSPAR Inf. Bul.*, 19–24, 2007.
- 688 Clerbaux, C., et al.: Monitoring of atmospheric composition using the thermal infrared IASI/MetOp
689 sounder, *Atmos. Chem. Phys.*, 9, 6041–6054, 2009.
- 690 Colon, J. A.: On interactions between the Southwest Monsoon Current and the Sea Surface over the
691 Arabian Sea, *Indian J. Met. Geophys.*, 15, 183 – 200, 1964.
- 692 Das, P.K.: *The Monsoons*, Nation Book Trust, New Delhi, India, ISBN 978-81-237-1123-2, 193,
693 2002.
- 694 Gadgil, S., and Joseph, P. V.: On breaks of the Indian monsoon, *Proc. Indian Acad. Sci.*, 112, 529–
695 558, 2003.
- 696 Kidder, S. Q., and Haar, T. H.V., Academic press inc., California, U.S.A.: *Satellite Meteorology -*
697 *An Introduction*, ISBN 0-12-406430-2, 199, 1995.
- 698 Kripalani, R. H., Kulkarni, S. A., Sabade, S., Revadekar, J. V., Patwardhan, S. K., and Kulkarni, J.
699 R.: Intra-seasonal oscillations during monsoon 2002 and 2003, *Curr. Sci.*, 87, 325– 331, 2004.
- 700 Kwon, E.H., Sohn, B. J., William, L., and Smith, J. L.: Validating IASI temperature and moisture
701 sounding retrievals over East Asia using radiosonde observations, *J. Atmos. Oceanic Technol.*, 29,
702 1250–1262, doi:10.1175/JTECH-D-11-00078.1, 2012.

703 Kursinski, E. R., Hajj, G. A., Schofield, J. T., Linfield, R. P. and Hardy, K. R.: Observing Earth's
704 atmosphere with radio occultation measurements using the Global Positioning System, *J. Geophys.*
705 *Res.*, 102, 23,429–23,466, doi:10.1029/97JD01569, 1997.

706 Lambriksen, B. H.: Calibration of the AIRS microwave instruments, *IEEE Trans. Geosci. Remote*
707 *Sens.*, 41, 369–378, 2003.

708 Narayanan, M. S., and Rao, B.M.: Detection of monsoon inversion by TIROS-N satellite, *Nature*,
709 294, 546 – 548, 1981.

710 Narayanan, M. S., and Rao, B. M.: Stratification and convection over Arabian Sea during monsoon
711 1979 from satellite data, *Proc. Indian Acad. Sci. (Earth Planet. Sci.)*, 98, 4, 339-352, 1989.

712 Narayanan, M. S., Rao, B.M. , Shah, S., Prasad, V. S., and Bhat, G.S.: Role of atmospheric stability
713 over the Arabian Sea and the unprecedented failure of monsoon 2002, *Current Science*, 86, 7, 938
714 – 947, 2004.

715 Rajeevan, M., and Bhate, J.: A high resolution daily gridded rainfall data set (1971–2005) for
716 mesoscale meteorological studies, *Curr. Sci.*, 96, 558– 562, 2009.

717 Rajeevan, M., Bhate, J., Kale, J. D., and Lal, B.: High resolution daily gridded rainfall data for the
718 Indian region: Analysis of break and active monsoon spells, *Curr. Sci.*, 91, 296– 306, 2006.

719 Ramage, C. S.: The Summer Atmospheric Circulation over the Arabian Sea, *J. Atmos. Sci.*, 23, 144
720 – 150, 1966.

721 [Roja Raman, M., Venkat Ratnam, M., Rajeevan, M., Jagannadha Rao, V.V.M., and Vijaya Bhaskara](#)
722 [Rao, S.: Intriguing aspects of monsoon low level jet over peninsular India revealed by high-](#)
723 [resolution GPS radiosonde observations, *J. Atmos. Sci.*, 68, 1413-1423, DOI:](#)
724 [10.1175/2011JAS3611.1, 2011.](#)

725 Sathiyamoorthy, V., Mahesh, C., Gopalan, K., Prakash, S., Shukla, B. P. and Mathur, A. K.:
726 Characteristics of low clouds over the Arabian Sea, *J. Geophys. Res.*, 118, 24, 13,489–13,503,
727 2013.

728 Schlüssel, P., Hultberg, T. H., Philipps, P. L., August, T., and Calbet, X.: The operational IASI level
729 2 processor, *Adv. Space Res.*, 36, 982–988, doi:10.1016/j.asr.2005.03.008, 2005.

730 Simmons, A. J., and Hollingsworth A.: Some aspects of the improvement in skill of numerical
731 prediction, *Q. J. R. Meteor. Soc.*, 128, 647–677, 2002.

732 Simmons, A., Uppala, S., and Dee, D.: Update on ERA-Interim, *ECMWF News L.*, 111, 5, 2007.

733 Simon, B., Rahman, S. H., Joshi, P. C. and Desai, P. S.: Shifting of the convective heat source over
734 the Indian Ocean region in relation to performance of monsoon: a satellite perspective, *Inter. J. of*
735 *Rem. Sens.*, 29:2, 387 – 397, doi: 10.1080/01431160701271966, 2007.

736 Smith, N., William L. Smith Sr., Elisabeth Weisz, and Henry E. Revercomb: AIRS, IASI, and CrIS
737 Retrieval Records at Climate Scales: An Investigation into the Propagation of Systematic
738 Uncertainty, *Am. Meteor. Soc.*, 54, 1565 – 1481, DOI: 10.1175/JAMC-D-14-0299.1, 2015.

739 Susskind, J., Barnet, C. D., and Blaisdell, J.M.: Retrieval of atmospheric and surface parameters
740 from AIRS/AMSU/HSB data in the presence of clouds, *IEEE Trans. Geosci. Rem. Sem.*, 41, 390-
741 409, 2003.

742 Thomas W. S.: An assessment of Operational TIROS – N Temperature Retrievals over the United
743 States, *Monthly Weather Review*, American Meteorological Society, 109, 110-119, 1981.

744 Wallace, J. M. and Hobbs, P. V., *International Geophysics series: Atmospheric Science - An*
745 *Introductory Survey*, Second Edition, 92, ISBN 13: 978-0-12-732951-2, 391, 2006,.

746 WMO, GARP Publication series no.18, *The Monsoon Experiment*, 1976.

747

748

749

750

751

752

753 **Figure captions:**

754 **Figure 1.** Typical examples showing MI in T and RH on (a) 27 June 1979 at 0730 GMT at 20°N,
755 60°E obtained from radiosonde from MONEX experiment, (b) same as (a) but at 0600 GMT from
756 ERA, (c) 30 July 2009 at 0514 GMT at 22°N, 68°E by IASI, (d) 30 July 2009 by ERA-Interim at
757 same location but at 0600 GMT. Note that scale for RH is shown in the top axis of (a) and (b).

758 **Figure 2.** Time series of ΔT for starting and ending of MI from April to October 2009 (black) and
759 2011 (blue). Green vertical lines are showing starting (01 May 2009) and ending (07 October 2009)
760 time for MI.

761 **Figure 3.** Base altitude occurrence of MI during (a) July, (b) August, ΔT (Strength) of MI (c) July,
762 (d) August, and Percentage occurrence of MI [days](#) (e) July, (f) August, averaged during 2009-2013
763 observed by IASI. (We are selecting WAS, CAS and EAS from this figure).

764 **Figure 4.** Percentage occurrence of (a) ΔT and (b) q at 700 hPa observed in WAS and EAS during
765 monsoon season of the years 2009-2013 for various ranges of ΔT and q at 700 hPa by IASI. (c) and
766 (d) same as (a) and (b) but obtained from ERA-Interim data.

767 **Figure 5.** Time series of (a) ΔT and (b) q at 700 hPa observed over WAS and EAS grid boxes
768 during the monsoon season of the year 2012 by IASI, (c) and (d) same as (a) and (b) but obtained
769 using ERA – Interim data. 3-point smoothed curves are shown.

770 **Figure 6.** MI observed in (a) ΔT and (b) q at 700 hPa during break spells (30 July – 11 August 2009)
771 of the year 2009 by IASI, (c) and (d) same as (a) and (b) but observed during active spells (14-17
772 July 2009). (e) and (f) and (g) and (h), same as (a) and (b) and (c) and (d) but observed by ERA-
773 Interim, respectively.

774 **Figure 7.** Time variations of (a) ΔT and (b) q at 700 hPa observed over WAS during two contrasting
775 years of 2009 and 2011 by using IASI measurements. Difference between 2011 and 2009 observed
776 in (c) ΔT and (d) q at 700 hPa. (e) to (h) same as (a) to (d) but observed by using ERA-Interim data
777 products.

778 **Figure 8.** Percentage occurrence of MI observed with (a) $\Delta T \leq 2K$ using IASI, AIRS and ERA-
779 Interim data during monsoon seasons of 2009-2013 over WAS and EAS.

780 **Figure 9.** Typical examples showing MI in temperature and RH on (a) 27 June 1979 at 0656 GMT at
781 $20^{\circ}N$, $62^{\circ}E$ obtained from dropsondes from MONEX experiment, (b) N profile (c) Scatter plot of
782 ΔT and ΔN .

783 **Figure 10.** Frequency of ΔN observed in Western AS and Eastern AS during monsoon season of the
784 years 2009-2013 for various ranges of ΔN by COSMIC. Western AS is showing higher
785 values means inversion is there.

786

787 **Table captions:**

788 **Table 1:** Data details for accuracy/error and availability.

789 **Table 2:** Comparison of aircraft profiles with satellite data.

790 **Table 1:** Data details for accuracy/error and availability.

	IASI	AIRS	COSMIC GPS - RO	ERA-Interim	MONEX 1979 In-situ data
Launch of satellite	MetOp – A launched in October 2006, 8461 spectral Channels	Aqua launched in May 2002, 2378 spectral channels	GPS – RO microsatellite receiver launched in April 2006	---	May – August 1979
Data availability from	August 2008	2003	April 2006	1979	May – August 1979
Data used in the present study	June – September 2009 - 2013	June – September 2009 – 2013	June – September 2009 - 2013	June – September 2009 - 2013	May – August 1979
Accuracy in Temperature	~ 1 K(RMS) at a vertical resolution of 1 Km(Clerbaux et al., 2007; 2009)	~ 1 K at a vertical resolution of 1 Km(Susskind et al., 2003)	Generally ~ 100m in the lower troposphere (not for T)	0.5 – 1.0 K at a vertical resolution of 0.8 – 1.0 km	± 1 °C in 4 vertical levels resolution(WMO report)
Accuracy in Humidity	~10 – 15 % accuracy with a 1 – 2 Km vertical resolution(Clerbaux et al., 2007; 2009)(Schlüssel et al., 2005)	~15 % accuracy with a 2 Km vertical layer resolution(Susskind et al., 2003)	---	~7.0 – 20 % at a vertical resolution of 0.8 – 1.0 km	± 30 % at a vertical resolution of 4 levels.
Accuracy in Refractivity	---	---	400 m to 1.4 km (Kursinski et al., 1997),		
Horizontal resolution	15 Km	25 Km	2000 soundings per day	1.5 ⁰ x 1.5 ⁰ (~ 80 km)	500 km
Pressure levels	1100- 0.0161 hPa - 100	1100 – 0.0161 hPa – 100	70% of occultations penetrate below 1 km (Anthes et al., 2008)	1013 – 1 hPa 37	1000 – 294 Different -2
Local equator crossing time	0930 LT descending node	1330 LT ascending node	-----	----	---
Swath	2200 km	1650 Km	-----		

791

792

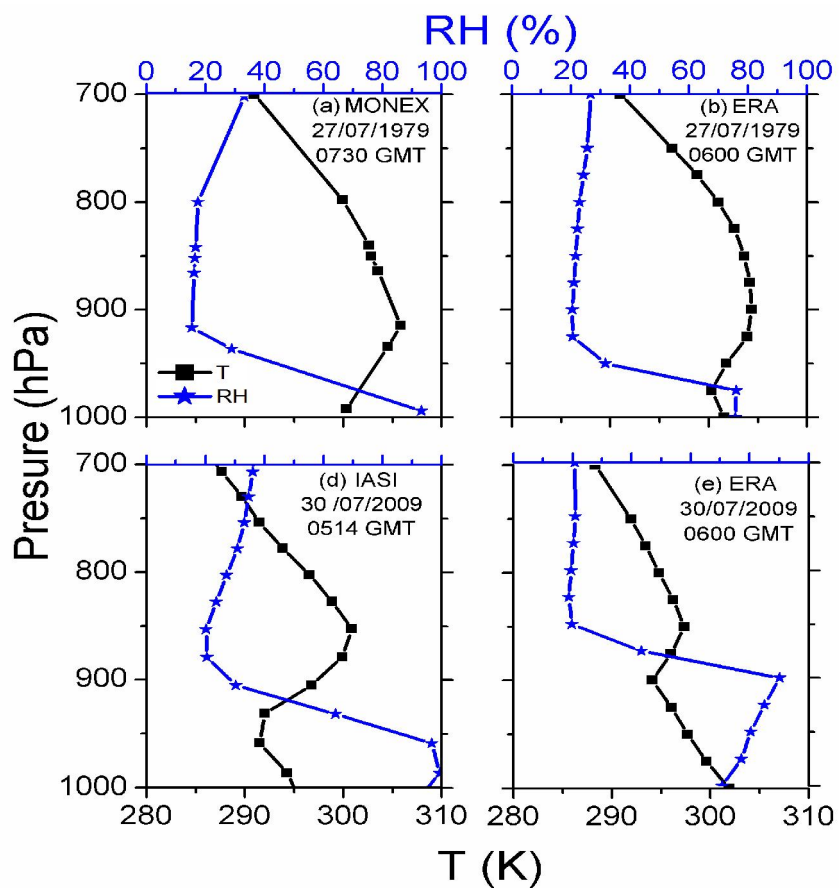
793 **Table 2:** Comparison of aircraft profiles with satellite data.

	Aircraft profiles	Near simultaneous satellite data	
		$\Delta T \leq 2^{\circ}\text{C}$	$\Delta T \geq 3^{\circ}\text{C}$
No. Of profiles with well – marked inversion below 850 mbar	30	23	7 (for four of them $\Delta T = 3^{\circ}\text{C}$)
No. Of profiles without well – marked inversion	129	0	129

794 (Regenerated from Narayanan et al., 1981)

795

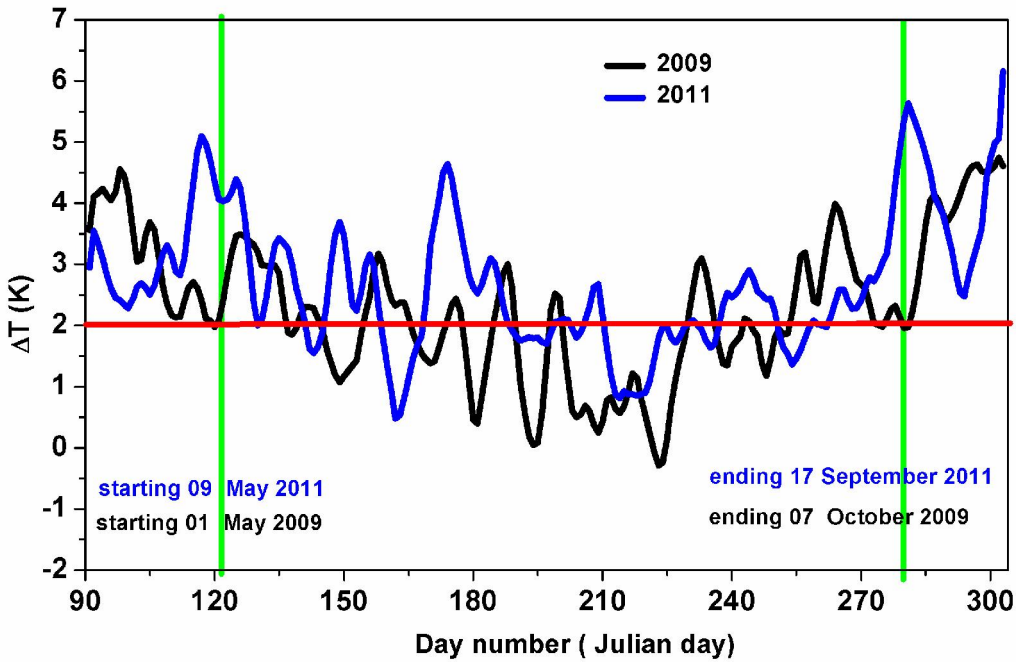
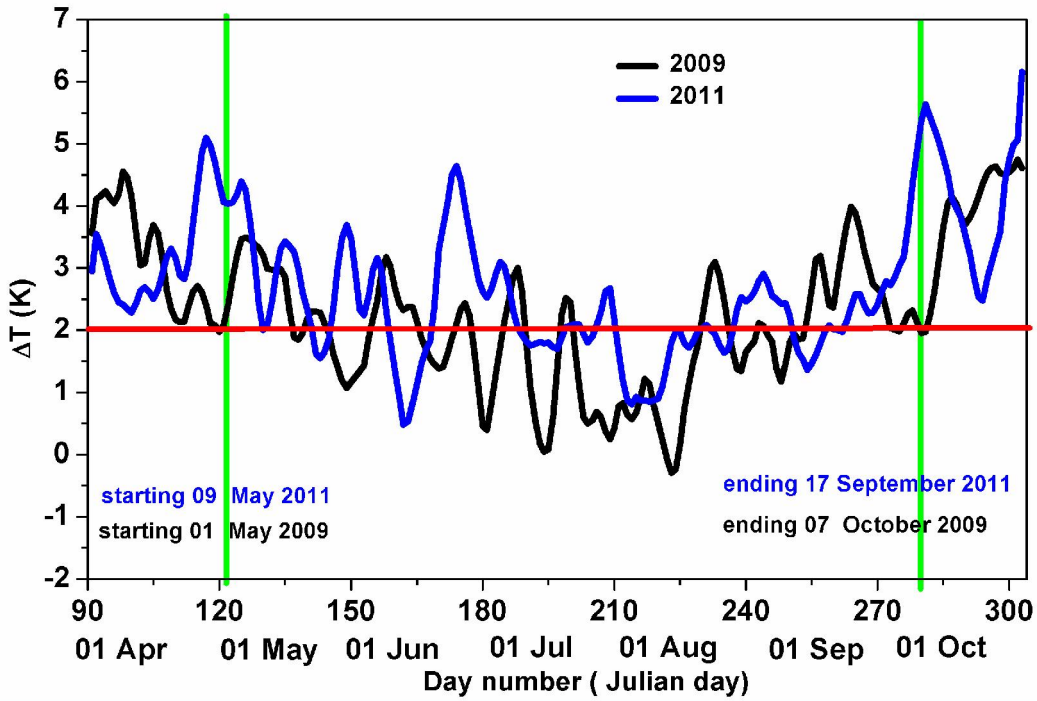
796 **Figures:**



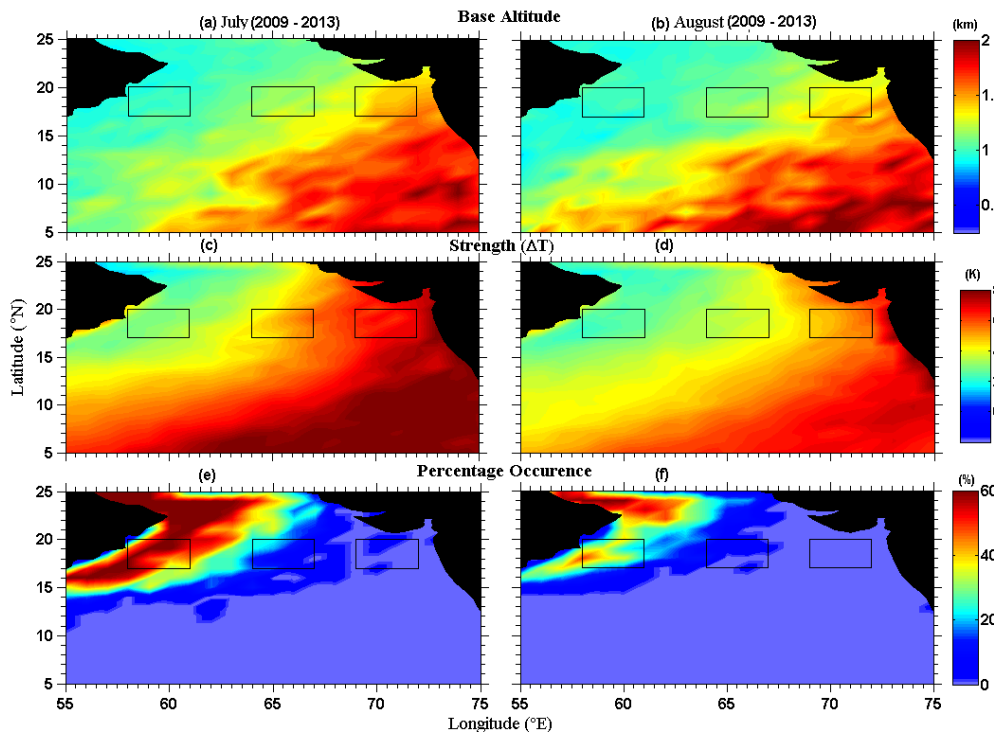
797

798 **Figure 1.** Typical examples showing MI in T and RH on (a) 27 June 1979 at 0730 GMT at 20°N,
799 60°E obtained from radiosonde from MONEX experiment, (b) same as (a) but at 0600 GMT from
800 ERA, (c) 30 July 2009 at 0514 GMT at 22°N, 68°E by IASI, (d) 30 July 2009 by ERA-Interim at
801 same location but at 0600 GMT. Note that scale for RH is shown in the top axis of (a) and (b).

Formatted: Font: Times New Roman, 12 pt



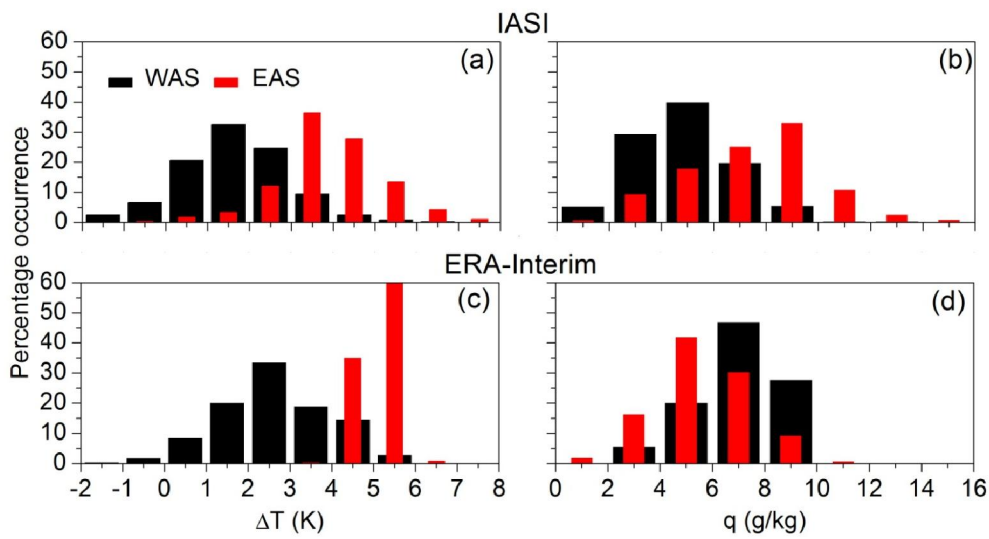
804 **Figure 2.** Time series of ΔT for starting and ending of MI from April to October 2009 (black) and
 805 2011 (blue). Green vertical lines are showing starting (01 May 2009) and ending (07 October 2009)
 806 time for MI.
 807



808 **Figure 3.** Base altitude occurrence of MI during (a) July, (b) August, ΔT (Strength) of MI (c) July,
 809 (d) August, and Percentage occurrence of MI [days](#) (e) July, (f) August, averaged during 2009-2013
 810 observed by IASI. (We are selecting WAS, CAS and EAS from this figure).
 811

812
 813
 814
 815
 816
 817

818
819
820
821
822

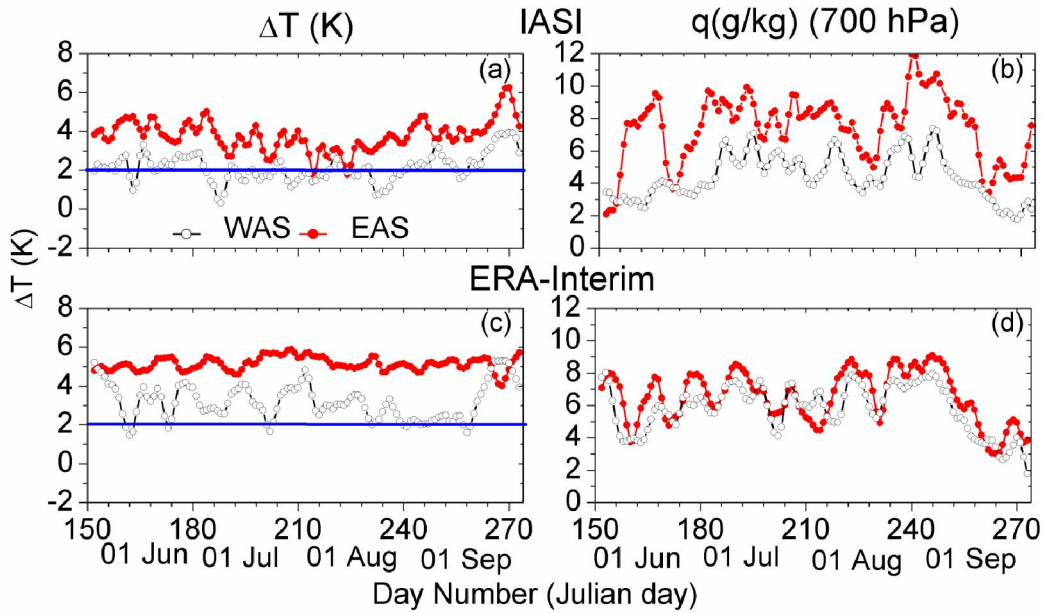


823
824
825
826
827
828
829
830
831
832
833
834

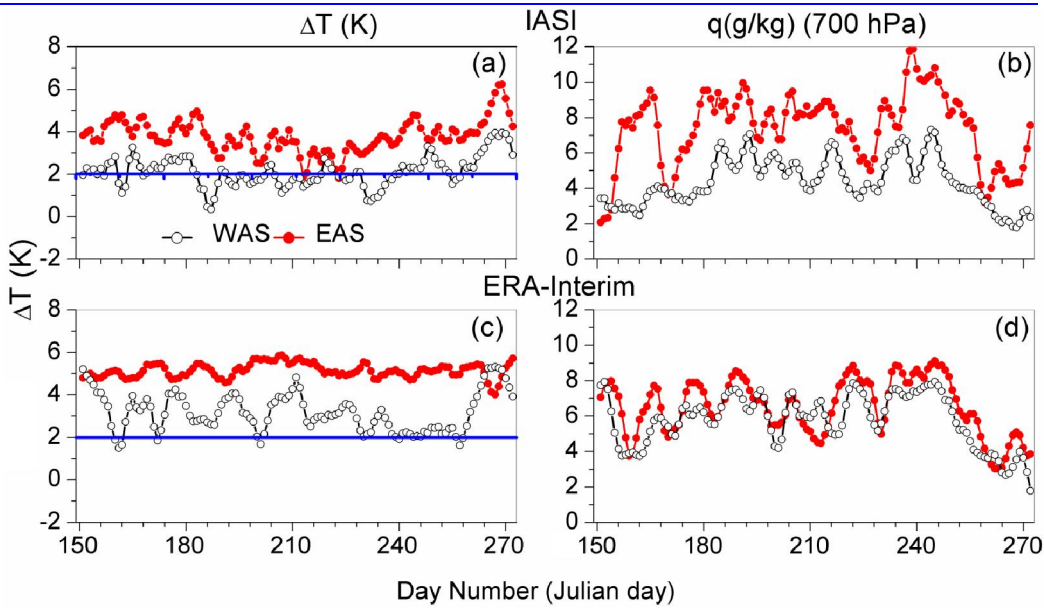
Figure 4. Percentage occurrence of (a) ΔT and (b) q at 700 hPa observed in WAS and EAS during monsoon season of the years 2009-2013 for various ranges of ΔT and q at 700 hPa by IASI. (c) and (d) same as (a) and (b) but obtained from ERA-Interim data.

835

836



837

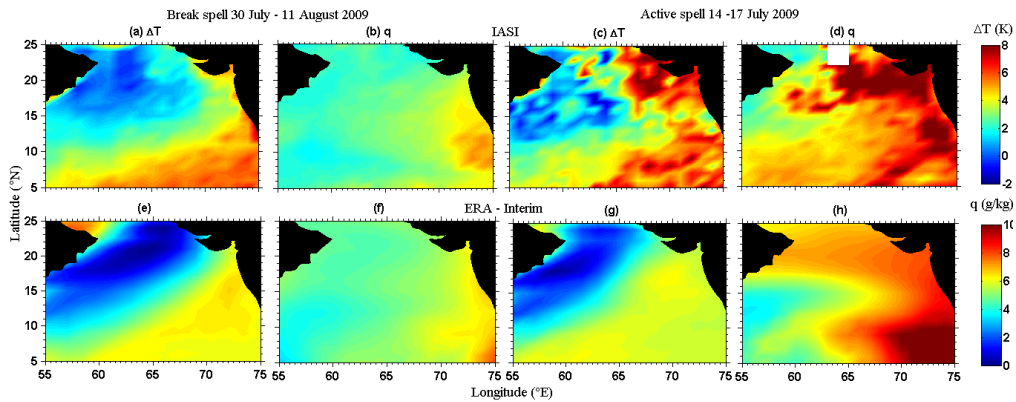


838

Formatted: Font: Times New Roman, 12 pt

839 **Figure 5.** Time series of (a) ΔT and (b) q at 700 hPa observed over WAS and EAS grid boxes
 840 during the monsoon season of the year 2012 by IASI, (c) and (d) same as (a) and (b) but obtained
 841 using ERA – Interim data. 3-point smoothed curves are shown.

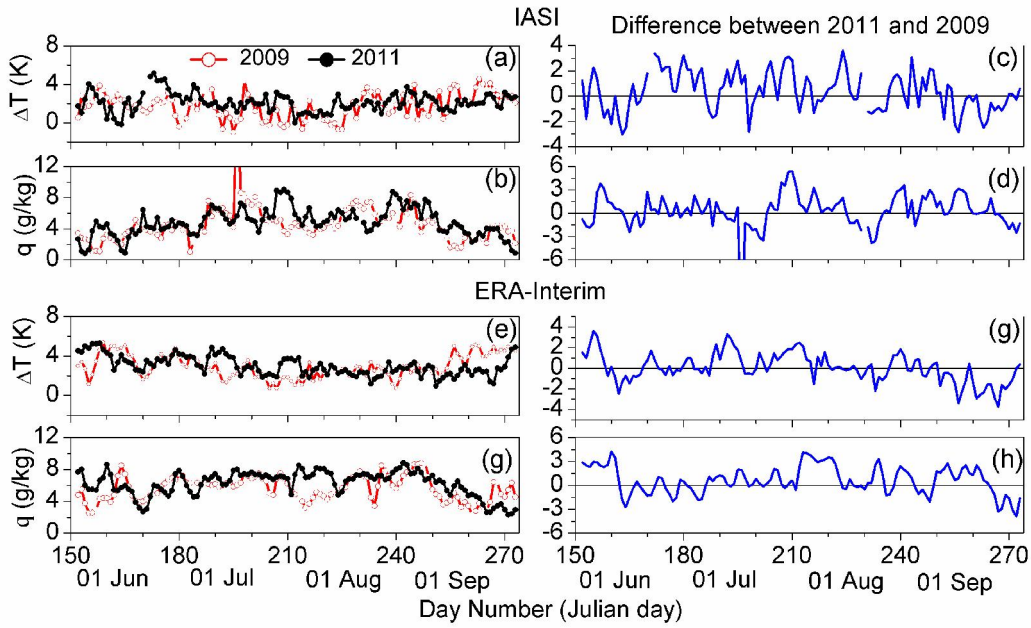
842
 843
 844
 845
 846
 847



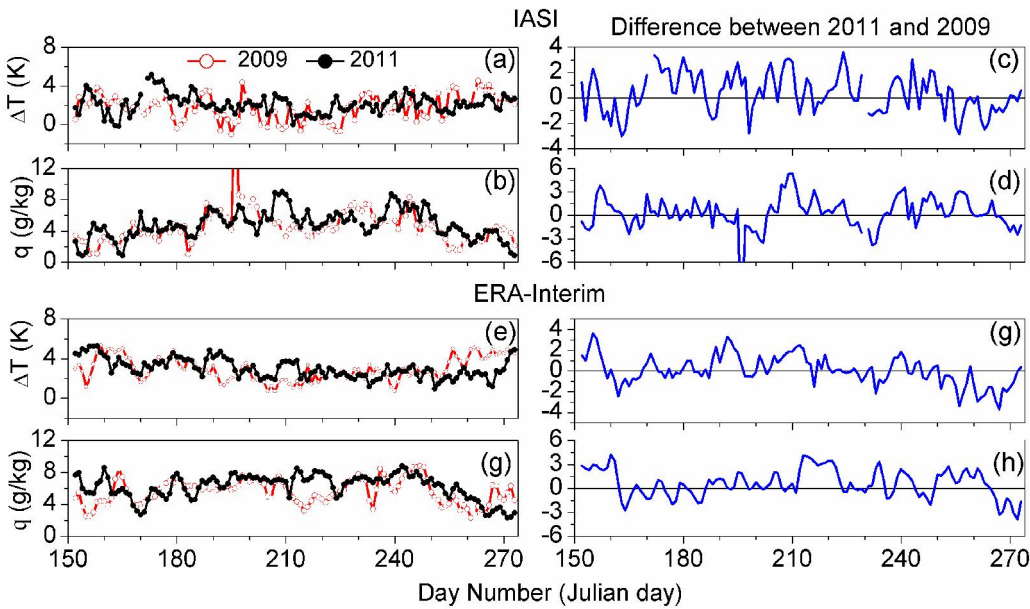
848 **Figure 6.** MI observed in (a) ΔT and (b) q at 700 hPa during break spells (30 July – 11 August
 849 2009) of the year 2009 by IASI, (c) and (d) same as (a) and (b) but observed during active spells
 850 (14-17 July 2009). (e) and (f) and (g) and (h), same as (a) and (b) and (c) and (d) but observed by
 851 ERA-Interim, respectively.

852
 853
 854
 855
 856
 857
 858

859
860
861



862



Formatted: Font: Times New Roman, 12 pt, Bold

863
864

Figure 7. Time variations of (a) ΔT and (b) q at 700 hPa observed over WAS during two

865 contrasting years of 2009 and 2011 by using IASI measurements. Difference between 2011 and
866 2009 observed in (c) ΔT and (d) q at 700 hPa. (e) to (h) same as (a) to (d) but observed by using
867 ERA-Interim data.

868

869

870

871

872

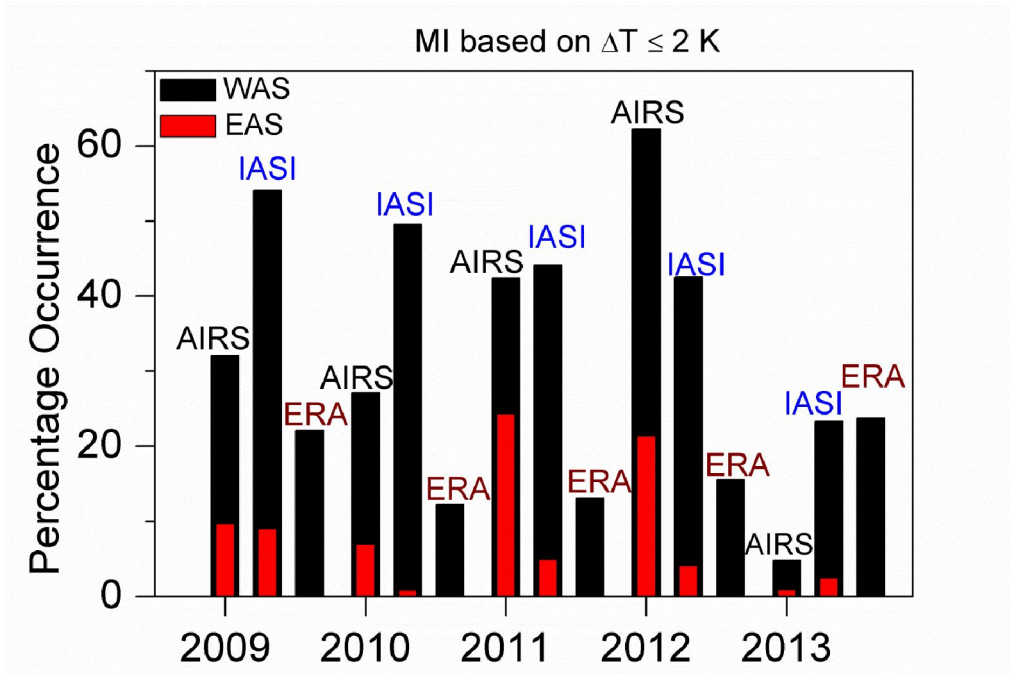
873

874

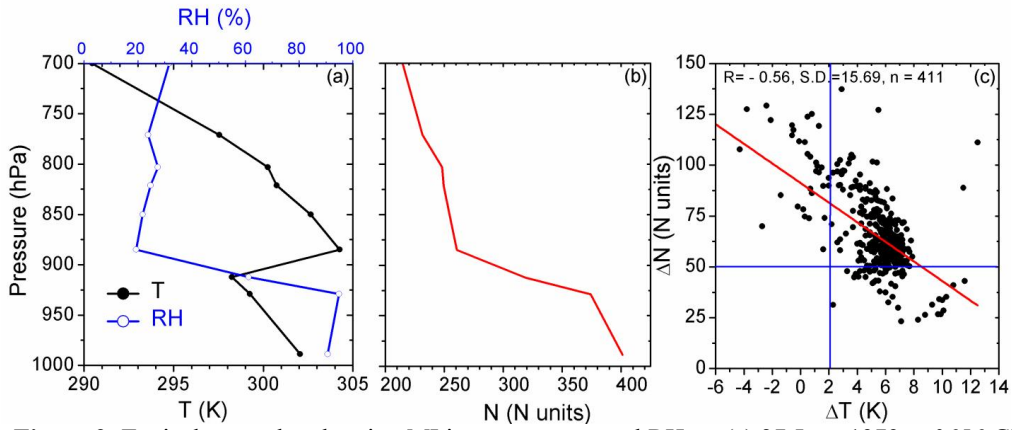
875

876

877



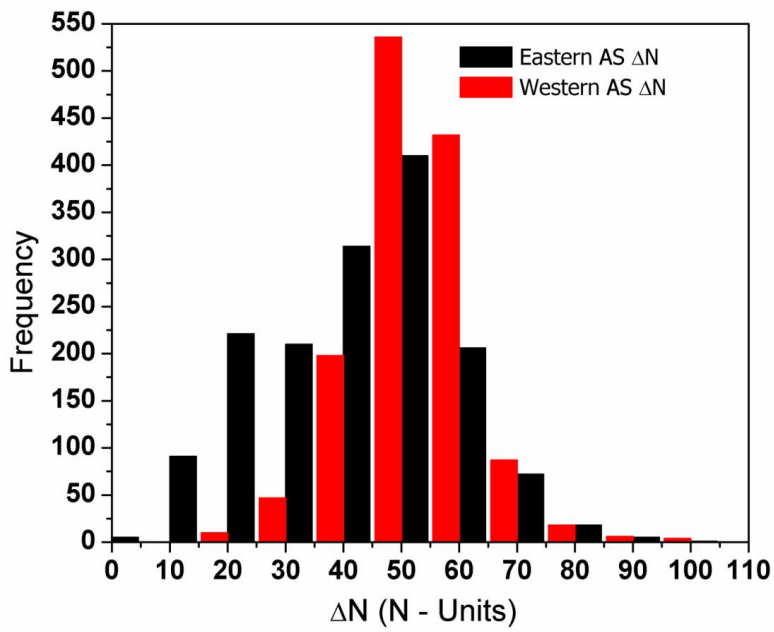
878 **Figure 8.** Percentage occurrence of MI observed with (a) $\Delta T \leq 2\text{ K}$ using IASI, AIRS and ERA-
 879 Interim data during monsoon seasons of 2009-2013 over WAS and EAS.
 880
 881
 882
 883
 884



885
 886 **Figure 9.** Typical examples showing MI in temperature and RH on (a) 27 June 1979 at 0656 GMT
 887 at 20°N, 62°E obtained from dropsondes from MONEX experiment, (b) N profile (c) Scatter plot of
 888 ΔT and ΔN .

889
 890
 891
 892
 893
 894
 895
 896
 897
 898
 899
 900
 901
 902
 903

904
905
906
907
908



909
910
911
912
913
914

Figure 10. Frequency of ΔN observed in Western AS and Eastern AS during monsoon season of the years 2009-2013 for various ranges of ΔN by COSMIC. Western AS is showing higher values means inversion is there.